

## Original Research

# Vaccine antibodies against a synthetic epidermal growth factor variant enhance the antitumor effects of inhibitors targeting the MAPK/ERK and PI3K/Akt pathways



Silvia García-Roman <sup>a</sup>, Mónica Garzón-Ibáñez <sup>a</sup>, Jordi Bertrán-Alamillo <sup>a</sup>, Núria Jordana-Ariza <sup>a</sup>, Ana Giménez-Capitán <sup>a</sup>, Beatriz García-Peláez <sup>a</sup>, Marta Vives-Usano <sup>a</sup>, Jordi Codony-Servat <sup>a</sup>, Erik d'Hondt <sup>b</sup>, Rafael Rosell <sup>c,d</sup>, Miguel Ángel Molina-Vila <sup>a,\*</sup>

<sup>a</sup> Laboratory of Oncology/Pangaea Oncology S.L., Dexeus University Hospital, C/ Sabino Arana 5, Barcelona 08023, Spain

<sup>b</sup> IN3BIO Europe Ltd, Aberdeen, UK

<sup>c</sup> Instituto Oncológico Dr. Rosell (IOR), Dexeus University Hospital, Barcelona, Spain

<sup>d</sup> Catalan Institute of Oncology and Institut d'Investigació en Ciències de la Salut Germans Trias i Pujol, Badalona, Spain

## ARTICLE INFO

## ABSTRACT

**Keywords:**  
EGF  
Vaccine  
Inhibitors  
Akt  
ERK

**Background:** The EGFR pathway is involved in intrinsic and acquired resistance to a wide variety of targeted therapies in cancer. Vaccination represents an alternative to the administration of anti-EGFR monoclonal antibodies, such as cetuximab or panitumumab. Here, we tested if anti-EGF antibodies generated by vaccination (anti-EGF VacAbs) could potentiate the activity of drugs targeting the ERK/MAPK and PI3K/Akt pathways.

**Methods:** Non-small cell lung cancer (NSCLC), colorectal cancer (CRC) and melanoma cell lines harboring KRAS, NRAS, BRAF and PIK3CA mutations were used. Anti-EGF VacAbs were obtained by immunizing rabbits with a fusion protein containing a synthetic, highly mutated variant of human EGF. Cell viability was determined by MTT, total and phosphorylated proteins by Western blotting, cell cycle distribution and cell death by flow cytometry and emergence of resistance by microscopic examination in low density cultures.

**Results:** Anti-EGF VacAbs potentiated the antiproliferative effects of MEK, KRAS G12C, BRAF, PI3K and Akt inhibitors in KRAS, NRAS, BRAF and PIK3CA mutant cells and delayed the appearance of resistant clones *in vitro*. The effects of anti-EGF VacAbs were comparable or superior to those of panitumumab and cetuximab. The combination of anti-EGF VacAbs with the targeted inhibitors effectively suppressed EGFR downstream pathways and sera from patients immunized with an anti-EGF vaccine also blocked activation of EGFR effectors.

**Conclusions:** Anti-EGF VacAbs enhance the antiproliferative effects of drugs targeting the ERK/MAPK and PIK3CA/Akt pathways. Our data provide a rationale for clinical trials testing anti-EGF vaccination combined with inhibitors selected according to the patient's genetic profile.

## Introduction

Treatment strategies for cancer patients have evolved significantly during the last two decades. Radio- and chemotherapy used to be the only therapies available in clinical practice for unresectable tumors; but response rates were generally low and toxicity issues often emerged, related to non-specific tissue distribution. Genomic profiling has revolutionized our understanding of carcinogenesis and has enabled the identification of the genes and proteins involved in tumorigenesis, including oncogenic drivers. Targeted drugs have been developed

against such drivers and have received approval for specific subsets of patients, selected based on the presence of specific genetic or epigenetic alterations. This precision medicine approach has improved response rates and survival outcomes in several malignancies [1].

The MAPK/ERK and PI3K/Akt signal transduction pathways play a key role in tumor progression, and alterations in the corresponding genes are oncogenic drivers in several malignancies. In the case of the MAPK/ERK pathway, driver mutations in the KRAS gene are present in 17 % of human tumors, being particularly prevalent in pancreas, colorectal (CRC), biliary tract, endometrium, ovary, and lung tumors [2].

\* Corresponding author.

E-mail address: [mamolina@panoncology.com](mailto:mamolina@panoncology.com) (M.Á. Molina-Vila).

Most mutations in the *KRAS* gene occur in codon 12, including p.G12C, frequent in smoking-associated non-small cell lung cancer (NSCLC); or p.G12V and p.G12D, common in CRC. Although driver alterations in *NRAS* and *HRAS* also appear in some malignancies; *BRAF* is the second most frequently mutated gene of the MAPK/ERK pathway, appearing in >50 % of melanoma and thyroid carcinoma and >10 % of CRC. Regarding the PI3K/Akt pathway, mutations in the *PIK3CA* gene, encoding the alpha subunit of the PI3K protein, are relatively common in human malignancies, particularly in breast and gynecological tumors [2]. However, most single *PIK3CA* mutations cannot completely activate the PI3K protein and are not generally considered as full drivers [3].

The relevance of the MAPK/ERK and PI3K/Akt/mTOR signal transduction in human cancer has prompted the development of antitumor drugs targeting different proteins of both pathways. Among the first of such agents to be approved, vemurafenib and dabrafenib were directed against mutant *BRAF* melanoma [4–6]. Several MEK inhibitors (MEKis), such as cobimetinib or trametinib, were also developed but failed to demonstrate clinical efficacy against *KRAS*-mutant tumors [7–9]. More recently, *KRAS* inhibitors targeting specific hotspot mutations have been developed and two of them, adagrasib and sotorasib, have received fast-track approval for treatment of G12C *KRAS*-mut NSCLC [10,11]. However, they show modest response rates, shorter progression-free survival and increased toxicities compared to other targeted agents used in NSCLC, such as EGFR or fusion-specific tyrosine kinase inhibitors (TKIs) [12,13]. Finally, several small molecules inhibiting PI3K, Akt or mTOR are in different stages of development and some of them are in clinical use. Two mTOR inhibitors, temsirolimus and everolimus, were approved as early as 2007–2011 for renal cell carcinoma [14,15] (RCC) while several PI3K inhibitors have received authorization for some hematological malignancies [16,17]. In contrast, no Akt inhibitors have been approved so far for clinical use [18].

Similarly to other targeted therapies, intrinsic and acquired resistance hamper the clinical efficacy of drugs inhibiting proteins of the MAPK/ERK and PI3K/Akt pathways. Combinations with other agents have been extensively tested to overcome resistance and some of them are in clinical use. MEKis were shown to improve response to *BRAF* inhibitors (*BRAF*is) and combined treatment is currently standard of care in *BRAF*-mut metastatic melanoma [19] and NSCLC [20]; while the PI3K inhibitor alpelisib has been approved with fulvestrant for hormone receptor (HR)-positive, *HER2*-negative, *PIK3CA*-mut breast cancer [21]. The EGFR and its ligands are involved in resistance to virtually all targeted agents [19,22–27], and combinations of the anti-EGFR monoclonal antibodies cetuximab and panitumumab with agents targeting MAPK/ERK and PI3K/Akt proteins have been tested in clinical trials. Two of those trials led to the approval of the *BRAF*i encorafenib combined with cetuximab for metastatic CRC patients carrying the *BRAF* V600E mutation [28,29].

Vaccination against EGF, one of the ligands of EGFR, represents an alternative to the administration of anti-EGFR monoclonal antibodies [30]. We have reported that anti-EGF antibodies generated by vaccination (anti-EGF VacAbs) significantly enhanced the antitumor effects of EGFR, ALK and RET TKIs in cells harboring *EGFR* mutations (*EGFR*-mut), *ALK* and *RET* translocations, respectively [31,32]. Based on this preclinical evidence, the EPICAL trial, a Phase Ib clinical trial combining afatinib with anti-EGF vaccination in *EGFR*-mut NSCLC patients, was initiated. The trial demonstrated that the vaccine is well tolerated, with a progression-free survival of 18 months to the combined treatment [33]; induces a robust immunogenic effect with high anti-EGF titers in patient's sera and effectively reduces the concentration in blood not only of EGF but also of TGF $\alpha$ , another relevant EGFR ligand. In this study, we aimed to determine if anti-EGF VacAbs could also improve the activity *in vitro* of drugs targeting the MAPK/Erk and PI3K/Akt pathways and delay the emergence of acquired resistance.

## Materials and methods

### Materials and cell lines

Anti-EGF VacAbs were obtained by immunizing rabbits with 4 injections of IN01, a recombinant fusion protein incorporating a synthetic EGF variant with mutations in several residues to enhance immunogenicity (Scotia Biologics Ltd., Aberdeen, UK), combined with Montanide adjuvant (Seppic, Paris, France). Sera from vaccinated animals were purified by Melon gel and treated with caprylic acid to remove contaminants. Pre-immunization sera from rabbit were also collected and purified to be used as control antibodies (Cabs). The anti-EGF VacAbs recognize and neutralize human EGF (hEGF) with high affinity, and the final preparation of purified anti-EGF VacAbs had a titer of 1:16,000 against hEGF by ELISA. This purified preparation was used in studies *in vitro* at dilution factors of 10 to 50, well below the anti EGF titers that can be reached in patients by vaccination [33].

Small molecule inhibitors used in the study (Supplementary Table 1) were purchased from Selleck Chemicals (Houston, TX) or MedChemExpress (Monmouth Junction, NJ), hEGF and antibodies for Western blotting from Cell Signaling Technologies (Beverly, MA) or other vendors (Supplementary Table 2). The range of concentrations tested systematically included those achieved in patients, according to pharmacokinetic studies.

Five NSCLC, four CRC and one melanoma cell line with different molecular alterations were used in the study (Supplementary Table 3). In the case of *KRAS*-G12C-mut NSCLC, we selected three cell lines with epithelial, intermediate, and mesenchymal phenotype, NCI-H358, NCI-H2122 and NCI-H23, respectively. All tissue culture materials were obtained from Gibco/Thermo Fisher Scientific (Paisley, Scotland, UK). Cell lines were maintained in Roswell Park Memorial Institute medium (RPMI) supplemented with 10 % fetal bovine serum (FBS), 50  $\mu$ g/mL penicillin-streptomycin and 2 mM L-Glutamine in a humidified atmosphere with 5 % CO<sub>2</sub> at 37 °C. Cells were weekly tested for mycoplasmas and authenticated by monthly genotyping for their driver alterations, *TP53* mutations and a panel of 4 polymorphisms. In the case of *KRAS*-G12C-mut NSCLC cell lines, we confirmed phenotypes by Western blot analysis of epithelial/mesenchymal markers (Supplementary Fig. 1). After no more than 15 passages, cells were discarded and a new, low-passage vial was thawed.

### Cell growth, viability, and emergence of resistant assays

To assess the effects of drugs, cells were seeded at different numbers (Supplementary Table 3) in 96-well plates and allowed to attach for 24 h in RPMI+10 % FBS. Then, they were washed twice with PBS and treated with 10 ng/mL of hEGF, antibodies, inhibitors, or combinations for 72 h in RPMI+0.5 % human serum (HS) except for the NCI-H2122 cells, which were treated in RPMI+2 % HS. After drug treatments, cells were incubated with medium containing 0.75 ng/mL Thiazolyl Blue Tetrazolium Bromide (MTT, Sigma Aldrich, St Louis, MO) for 1–2 h at 37 °C. Culture medium was removed; formazan crystals reabsorbed in DMSO (Merck, Darmstadt, Germany) and cell numbers estimated by reading the A<sub>565</sub> using an Infinite M Plex Tecan microplate reader (Männedorf, Switzerland). For determination of growth curves, cells were seeded at different numbers (Supplementary Table 3), cultured up to 16 days and cell viability estimated by with MTT as explained above. Data were derived from at least three independent experiments, normalized with the A<sub>565</sub> obtained for control cells (growing in absence of drugs or hEGF) and presented as mean  $\pm$  SEM.

To study the acquisition of resistance, 350 cells per well were seeded in 96-well plates. Cells were allowed to attach, and treatments were started after 24 h in RPMI+10 % FBS. Media was changed every week, plates were inspected thrice a week under the microscope, and wells >50 % confluent were scored as positive. After the emergence of HT29 resistant clones to encorafenib (ER), encorafenib combined with

cetuximab (ECR) and encorafenib with anti-EGF VacAbs (EAR), we isolated and characterized at the DNA, RNA, and protein levels ten colonies per treatment. Colonies were selected at different timepoints (early, intermediate, and late) after initiating the treatment; 10, 18 and 22 days for ER; 10, 31 and 55 days for ECR and 10, 55 and 97 days for EAR.

#### Western blot analysis

Subconfluent cultures were treated in T-25 or T-75 flasks with hEGF (10 ng/mL), CAbs, anti-EGF VacAbs, inhibitors or combinations, in RPMI+0.5 % HS. After washing twice with cold PBS, cultures were scraped into RIPA buffer (20 mM Tris-HCl pH 7.5, 150 mM NaCl, 1 mM Na<sub>2</sub>EDTA, 1 mM EGTA, 1 % NP-40, 1 % sodium deoxycholate, 2.5 mM sodium pyrophosphate, 1 mM β-glycerophosphate, 1 mM Na<sub>3</sub>VO<sub>4</sub>, 1 μg/mL leupeptin (Cell Signaling Technologies), 2 mM PMSF and Protease Inhibitor Cocktail (Roche Diagnostics, Mannheim, FRG)) and passed through an insulin syringe. Lysates were incubated on ice 10 min, centrifuged for 10 min at 14,000 rpm and immediately analyzed or snap frozen at -80 °C. Protein extracts (20–40 μg) were boiled in Laemmli buffer (NuPAGE- LDS sample buffer 4X; Invitrogen, Carlsbad, CA), resolved in SDS-polyacrylamide gels and transferred to PVDF membranes (Bio-Rad, Hercules, CA). Membranes were incubated for 1 h in Phosphoblocker reagent (Cell Biolabs Inc, San Diego, CA), cut, incubated with primary antibodies (Supplementary Table 2) o/n at 4 °C, washed three times with PBS-Tween 0.1 % and incubated for 2 h with a secondary antibody (Supplementary Table 2). Finally, membranes were washed with PBS-Tween 0.1 %, revealed with Supersignal Chemiluminescence substrate (Thermofisher, Waltham, MA) and read with a Bio-Rad ChemiDocMP Imaging System.

#### Flow cytometry

Cultures were treated under the same conditions described for Western blotting, trypsinized and centrifuged. For cycle analyses, cells were resuspended in PBS, fixed in 70 % ethanol, incubated o/n at -20 °C, centrifuged at 1200 rpm for 5 min at 4 °C, incubated for 1 h at 37 °C in 250 μL of PBS with 50 mg/mL RNase A (Sigma Aldrich) and stained with propidium iodide (PI) for 30 min at room temperature in the dark. For cell death analyses, the Annexin-V FLUOS staining kit (Roche Diagnostics) was used according to the manufacturer's instructions. Stained cells were analyzed with a FACSCanto II cytometer (BD Biosciences, Franklin Lakes, New Jersey) using the FACSDiva software version 6.1.2. In the case of cell death analyses, the combination of annexin V and PI was used to differentiate four cell populations: namely, viable cells (An-/PI-), early apoptotic (An+/PI-), necrotic (An-/PI+), and later apoptotic/necrotic (An+/PI+).

#### DNA purification and NGS sequencing analysis

For DNA purification of cell lines, we used the DNeasy Blood & Tissue Kit (QIAGEN, Hilden, Germany), following the manufacturer's instructions. DNA concentration was measured by Qubit® and samples with DNA ≥ 2.5 ng/μL were diluted to this concentration. DNA-based next generation sequencing (NGS) was performed, according to the manufacturer's instructions, with the GeneRead® QIAact Custom extended Panel (Qiagen, Hilden, Germany), which can detect mutations and copy number variations in *EGFR*, *BRAF*, *MET*, *ERBB2*, *ALK*, *ROS1*, *PIK3CA*, *KRAS*, *NRAS*, *FGFR1*, *FGFR2*, *FGFR3*, *KIT*, *PDGFRA*, *TP53*, *CDK4*, *CDK6*, *IDH1*, *IDH2*, *ERBB4*, *STK11*, *MYC*, *RET*, *POLE*, *POLD1*, *KEAP1*, *ARID1A*, *FAT1*, *NFE2L2* and *SETD2*. Up to 40 ng of purified DNA were used as a template. Clonal amplification was performed on pooled libraries (625 pg) and, following bead enrichment, the GeneReader instrument was used for sequencing. Qiagen Clinical Insight Analyze (QCI-A) software was employed to align the read data and call sequence variants, which were imported into the Qiagen Clinical Insight Interpret

(QCI-I) web interface for data interpretation and generation of final custom report.

#### RNA extraction and NanoString® nCounter assay

The High Pure RNA isolation Kit (Roche Diagnostics) was employed for RNA extraction from ER, ECR and EAR colonies according to the manufacturer's instructions, and concentrations were estimated using the Qubit 3.0 fluorometer (Invitrogen, Eugene, OR, USA). Purified RNA was analyzed using the nCounter® PanCancer Pathways Panel (NanoString Technologies, Seattle, WA), which includes 730 transcripts and 40 housekeeping genes. The hybridization steps were performed in a Verity thermal cycler (Applied Biosystems, South San Francisco, CA, USA). All processes of capture, cleanup, and digital data acquisition were performed with nCounterPrep StationTM and Digital AnalyzerTM (NanoString Technologies, Seattle, WA, USA) according to the manufacturer's instructions. The number of counts for each gene was extracted from the nCounter generated RCC files using nSolver analysis Software (version 4.0.70 NanoString Technologies) and exported to Microsoft Excel software. RNA counts were normalized using the positive controls and housekeeping transcripts, as described [34]. Finally, pathway analysis was performed using nCounter Advanced Analysis 2.0 from nSolver and STRING free software version 11.5 [35]. Only pathways identified by both methods in the same colony were considered.

#### Human sera and ELISAs

Sera from patients enrolled in the BV-NSCLC-001 clinical trial (NCT01444118) were kindly provided by InBio Europe Ltd. BV-NSCLC-001 was a randomized trial to study the safety and efficacy of anti-EGF VacAbs in late-stage (IIIB/IV) NSCLC patients, who were immunized with a first generation anti-EGF vaccine [30,31]. All patients provided written and informed consent. The concentration of hEGF in sera was assayed using the Quantidine ELISA hEGF immunoassay (R&D systems, Minneapolis, MN), according to the manufacturer's instructions. The titer of anti-EGF VacAbs in rabbit and patient's sera were determined using an in-house ELISA. Briefly, recombinant hEGF (2 μg/mL) (Sigma-Aldrich) was attached to the wells of a flat bottom 96-wells plate, wells were blocked, incubated with serial dilutions of patient's sera followed by goat anti-rabbit antibodies conjugated with horseradish peroxidase (Sigma-Aldrich). In head-to-head comparisons of anti-EGF VacAbs with cetuximab and panitumumab, the same protein concentrations were used. Finally, a substrate solution was added for 20 min, the reaction stopped with 1 N NaOH (Macron Fine Chemicals, Radnor, PA) and plates read at 405 nm with Infinite M Plex microplate reader.

#### Results

##### Anti-EGF VacAbs suppressed the stimulatory effects of hEGF in cell lines with KRAS, NRAS, and BRAF mutations

First, we tested the effects of hEGF at 10 ng/mL on the *KRAS* (*n* = 6), *NRAS* (*n* = 1) and *BRAF* (*n* = 3) tumor cell lines selected for our study, some of which harbored concomitant mutations in *PIK3CA* (*n* = 3) (Supplementary Table 3). In five of the lines, the addition of hEGF for 72 h to cells growing in 0.5 % human serum significantly stimulated growth. Particularly interesting were the cases of the *BRAF*-mut H508 and WM115 cells, where the effect reached 40 % (Supplementary Fig. 2). Dose-response experiments revealed that anti-EGF VacAbs were able to block the proliferative effects of hEGF, whereas CAb showed no activity (Supplementary Fig. 3). Western blotting experiments were subsequently performed in *KRAS*, *NRAS* and *BRAF*-mut cells to determine the activation of EGFR downstream pathways. As expected, hEGF at 2 h induced the phosphorylation of EGFR in all the cell lines tested, accompanied with activation of ERK1/2 and/or Akt. The addition of anti-EGF VacAbs consistently blocked hEGF-induced phosphorylation of

EGFR, together with ERK1/2 and/or Akt, while CAbs had no effect (Supplementary Fig. 4). As observed in case of the proliferation experiments, the effects of hEGF and anti-EGF VacAbs were apparent independently of the type of mutation harbored by the cells.

**hEGF significantly reduced the antiproliferative effects of drugs targeting the MAPK/ERK and PI3K/Akt pathways in tumor cells**

Next, we used our panel of cell lines to investigate whether hEGF altered the antiproliferative effects of small molecule inhibitors targeting proteins of the MAPK/ERK and PI3K/Akt pathways. In cell viability experiments, we found that the addition of hEGF to the culture medium significantly reduced the activity of trametinib, binimetinib, sotorasib, encorafenib, dabrafenib, vemurafenib, alpelisib, capivasertib, copanlisib and taselisib in *KRAS*, *NRAS* and *BRAF*-mut cells, some of them harboring concomitant *PIK3CA* mutations. As a result, we observed significantly higher IC<sub>50</sub>s and percentage of surviving cells after treatment in presence of hEGF (Supplementary Figs. 5–7, Table 1, Supplementary Table 4).

Western blotting experiments, in presence of hEGF, revealed that the MEKi trametinib and the KRAS-G12C inhibitor (G12Ci) sotorasib inhibited ERK1/2 activation at concentrations >1–100 nM in *KRAS*, *NRAS* and *BRAF*-mut cells. As expected, trametinib and sotorasib had limited or no effects on the levels of phosphor-EGFR (pEGFR) and phosphor-Akt (pAkt)/phosphor-PRAS40 (Supplementary Fig. 8). In contrast, when hEGF was present, the BRAF inhibitors encorafenib, dabrafenib and vemurafenib failed to block ERK1/2 or Akt/PRAS40 phosphorylation in *BRAF*-mut cells at concentrations as high as 1 μM. Finally, the PI3K and AKT inhibitors alpelisib, copanlisib, taselisib and capivasertib abolished Akt activation at 10–500 nM in the *PIK3CA*-mut NCI-H508 and DLD1 cells, showing weaker or no effects on pERK1/2 or pEGFR levels (Supplementary Fig. 9).

**Anti-EGF VacAbs enhanced the activity of inhibitors targeting the MAPK/ERK and PI3K/Akt pathways, outperforming cetuximab in *BRAF*-mut CRC cells**

Next, we tested if anti-EGF VacAbs could reverse the effect of hEGF and, consequently, increase the antitumor effects of small molecule inhibitors of the MAPK/ERK and PI3K/Akt pathways. The anti-EGF VacAbs had been raised by immunizing rabbits with IN01, a recombinant protein incorporating a synthetic, highly mutated EGF variant, as explained in Methods. Viability assays at 72 h in presence of hEGF revealed that the addition of anti-EGF VacAbs significantly enhanced the efficacy of the MEKi trametinib and binimetinib in *KRAS* and *NRAS*-mut tumor cells, with a >10-fold reduction in IC<sub>50</sub>s in 4/5 cell lines tested. In contrast, the antibodies showed a more modest effect in the activity of MEKi against *BRAF*-mut cells, particularly in the case of trametinib, where the decrease in IC<sub>50</sub> was <10-fold in the three lines analyzed. In the case of the G12Ci sotorasib, the IC<sub>50</sub>s dropped 10 to >10,000 fold in presence of anti-EGF VacAbs in the three *KRAS*-mut G12C cell lines tested, while the effects of the antibodies on sensitivity to BRAFi were widely different in the two *BRAF*-mut lines used. Viability assays revealed a 50–1000-fold decrease in the IC<sub>50</sub> to encorafenib, dabrafenib and vemurafenib in the HT29 colon cells, compared to a <3-fold reduction in the WM793 melanoma cells. Finally, a moderate impact of the addition of anti-EGF VacAbs was observed for the PI3K/AKT inhibitors alpelisib, capivasertib, copanlisib and taselisib, with <4-fold changes of the IC<sub>50</sub>s in *PIK3CA*-mut cells. As expected, CAbs showed no significant activity in any case (Fig. 1, Supplementary Figs. S10–11, Table 1).

As mentioned, in the case of the HT29 cell line we observed a particularly significant potentiation by anti-EGF VacAbs of the antiproliferative effects of BRAFi. This finding prompted us to compare the anti-EGF VacAbs head-to-head with cetuximab; the anti-EGFR monoclonal antibody currently approved for clinical use in *BRAF*-mut CRC, in combination with encorafenib [28,29]. Remarkably, when combined

**Table 1**

Effects of hEGF at 10 ng/mL and the anti-EGF VacAbs (1/25 dilution in presence of hEGF) on the sensitivity of MEK1/2, KRAS, BRAF, PIK3CA and AKT inhibitors. Cells were grown in medium plus 0.5 % HS with/without 10 ng/mL hEGF. The IC<sub>50</sub> values are referred to control wells where hEGF, inhibitors and Ab were absent. In *KRAS*-mut cell lines the anti-EGFR antibody used was panitumumab while in the *BRAF*-mut cell lines we used cetuximab. C-Ab, control anti-EGF VacAb; Ab, anti-EGF VacAb; I, inhibitor. *KRAS* and *NRAS*-mut cells are indicated in bold, the rest are *BRAF*-mut cells.

Inhibitor	Cell line	IC <sub>50</sub> s (nM) w/o hEGF		IC <sub>50</sub> (nM) in presence of hEGF (10 ng/mL)		I + anti-EGFR Ab
		I	I + C-Ab	I	I + Ab	
Trametinib	<b>A549</b>	48.7		1659.6	>2500.0	131.8
	<b>DLD1</b>	453.5		2187.8	1548.8	104.7
	<b>NCI-H23</b>	52.3		2494.6	1548.8	151.4
	<b>NCI-H508</b>	870.2		407.4	407.4	162.2
	<b>HCC15</b>	491.2		>50,000.0	>50,000.0	776.2
	HT29	6.9		50.1	50.1	4.6
	LS174T	7.4		104.7	104.7	38.9
	WM115	1802.8		>5500.0	>5500.0	5128.6
	<b>DLD1</b>	6125.7		35,481.3	35,481.3	6309.6
Binimetinib	<b>NCI-H23</b>	5000.0		>5000.0	>5000.0	933.3
	<b>HCC15</b>	80.1		724.4	776.2	43.7
	HT29	201.7		2290.9	1445.4	30.0
	LS174T	136.5		>1000.0	>1000.0	70.8
	WM115	>5000.0		>5500.0	>5500.0	5000.0
Sotorasib	<b>NCI-H2122</b>	612.5		>25,000.0	>25,000.0	0.001
	<b>NCI-H23</b>	12,500.0		>50,000.0	>50,000.0	616.6
	<b>NCI-H358</b>	2.4		85.1	74.1	9.7
Encorafenib	HT29	2.5		>2500.0	>2500.0	4.9
	WM115	4760.2		>5500.0	>5500.0	5011.9
Dabrafenib	HT29	48.9		>5000.0	>5000.0	6.1
	WM115	>10,000.0		>10,000.0	>10,000.0	6982.3
Vemurafenib	HT29	500.2		>5000.0	>5000.0	151.4
	WM115	2892.8		5546.3	5546.3	1380.4
Alpelisib	<b>NCI-H508</b>	9125.8		6165.9	9549.9	3019.9
	<b>NCI-H508</b>	3326.8		11,749.0	8709.6	3548.1
Capivasertib	<b>NCI-H508</b>	122.4		616.6	831.8	154.9
	<b>DLD1</b>	8875.3		19,054.6	17,378.0	631.0
Taselisib	<b>NCI-H508</b>	251.4		616.6	1023.3	41.7

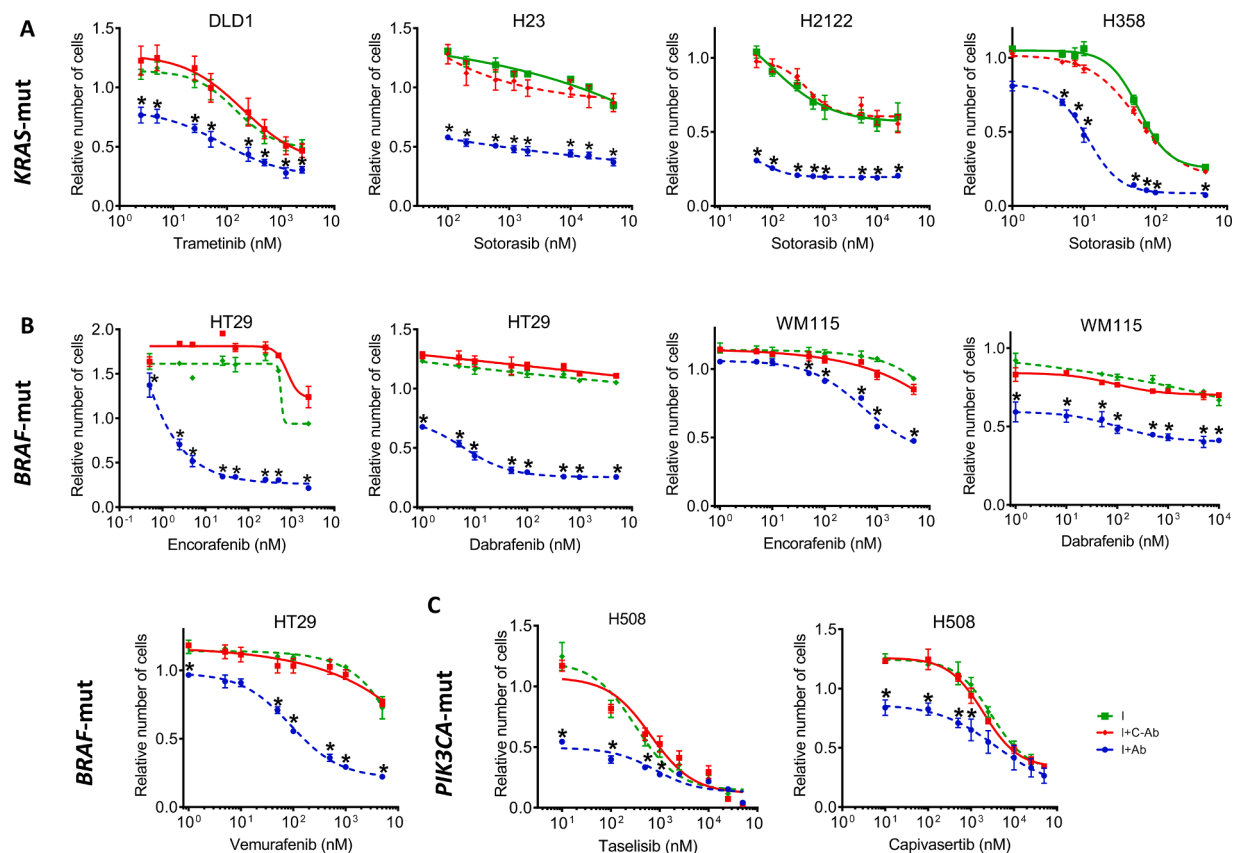


**Fig. 1.** Effects of anti-EGF VacAbs combined with inhibitors targeting the MAPK/ERK and PI3K/Akt pathways in mutant cell lines. Dose-response plots after 72 h treatments in (A) KRAS-mut, (B) BRAF-mut and (C) PIK3CA-mut cells. Medium was RPMI+0.5 % HS with 10 ng/mL of hEGF in all cases. Data were pooled from at least three different experiments and presented as mean  $\pm$  SEM. \*,  $P < 0.05$  compared to C-Ab (Student's t-test). Ab, anti-EGF VacAbs; C-Ab, control antibodies; I, inhibitor.

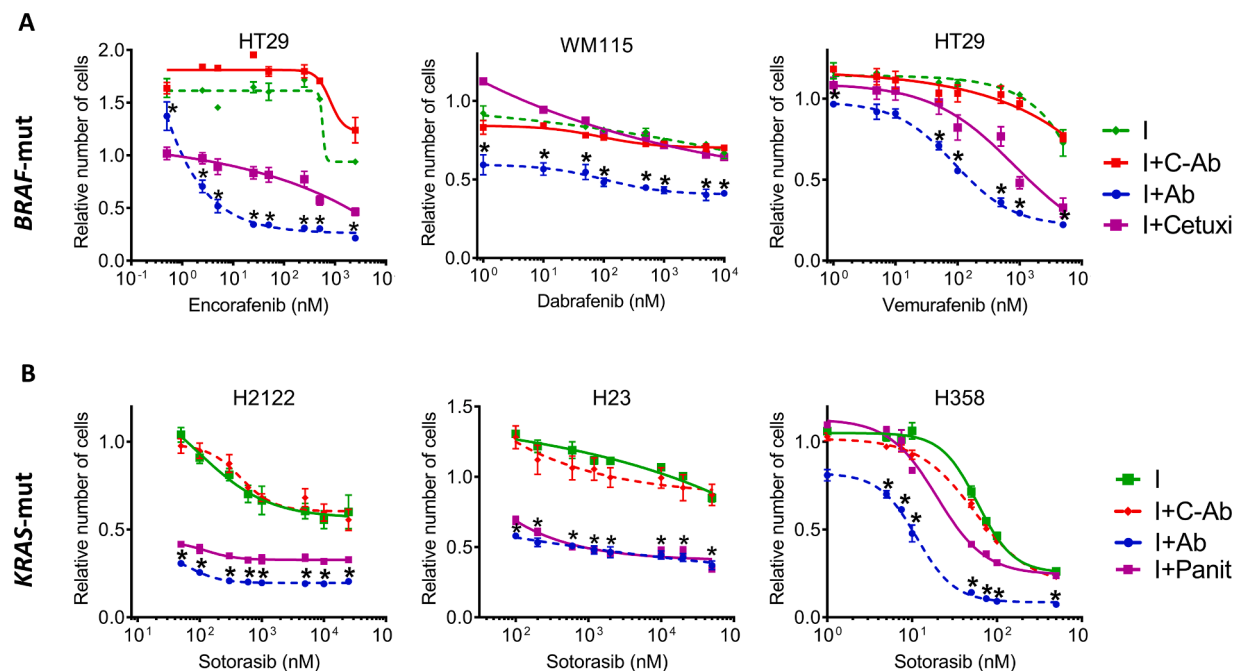


**Fig. 2.** Effects of inhibitors targeting the MAPK/ERK and PI3K/Akt pathways combined with antibodies in BRAF and KRAS mutant cell lines. Dose-response plots after 72 h treatments in (A) BRAF-mut and (B) KRAS-mut cell lines. Medium was RPMI+0.5 % HS with 10 ng/mL of hEGF in all cases. Data were pooled from at least three different experiments and presented as mean  $\pm$  SEM. \*,  $P < 0.05$  compared to C-Ab (Student's t-test). Ab, anti-EGF VacAbs; C-Ab, control antibodies; Cetuxi, cetuximab; I, inhibitor; Panit, panitumumab.

with encorafenib, dabrafenib and vemurafenib, the anti-EGF VacAbs outperformed cetuximab at most concentrations tested, not only in CRC HT29 but also in the melanoma WM793 cells (Table 1, Fig. 2A). In addition, sotorasib is currently being tested with panitumumab in clinical trials, which have reported promising preliminary results [36]. Consequently, we also compared head-to-head anti-EGF VacAbs vs. panitumumab in combination with sotorasib, using three G12C cell lines. We found that anti-EGF VacAbs were more potent than panitumumab in NCI-H358 and NCI-H2122 cells, while results were indistinguishable in NCI-H23 (Table 1, Fig. 2B).

Growth curves of KRAS, NRAS, BRAF and PIK3CA cell lines up to 8–16 days confirmed a significant reduction in the activity of trametinib, binimetinib, sotorasib, vemurafenib, dabrafenib, alpelisib, copanlisib, taselisib and capivasertib in KRAS, NRAS and BRAF-mut cells when hEGF was present (Supplementary Figs. 12 and 13). In addition, an experiment using different concentrations of the growth factor combined with encorafenib showed that the effect was dose-dependent and could be observed at concentrations as little as 0.5 ng hEGF/mL (Supplementary Fig. 13B). When anti-EGF VacAbs were added, the deleterious effects of hEGF were reversed in all cell lines tested and, in consequence, the antiproliferative activity of the drugs targeting the MAPK/ERK and PI3K/Akt pathways was significantly enhanced. The anti-EGFR monoclonal antibody panitumumab, when tested in combination with sotorasib, showed similar effects (Fig. 3A-C, Supplementary Fig. 14A).

**Anti-EGF VacAbs in combination with inhibitors targeting the MAPK/ERK and PI3K/Akt pathways efficiently blocked the corresponding pathways in tumor cell lines**

Cell cycle and Annexin V experiments were subsequently performed to gain insight in the cell cycle alterations responsible for the results obtained in proliferation assays. In the case of HT29, we observed that the BRAFi encorafenib significantly reduced the percentage of cells in S + G2/M and triggered cell death, as expected. The addition hEGF reversed these effects, while anti-EGF VacAbs blocked the effects of hEGF, enhancing the drug-induced cell cycle arrest and cell death (Fig. 3D-E, Supplementary Fig. 15). Similar results were obtained in cell cycle experiments testing the combination of trametinib with anti-EGF VacAbs in the KRAS-mut cells A549 and DLD1 (Supplementary Fig. 14B).

Next, we used Western Blotting to analyze the effects of inhibitors, hEGF and anti-EGF VacAbs in key signal transduction proteins of the MEK/Erk and Akt pathways (Fig. 4, Supplementary Figs. 16–17). We found that the addition of hEGF increased the levels of pEGFR and pERK1/2 in the KRAS-mut A549, H23, H2122 and LS174T cells; the NRAS-mut HCC15 cells and the BRAF-mut HT29 and WM115 cells (i.e., Fig. 4, compare lanes #1 and #2). We also observed that the presence of hEGF blocked the inhibitory effects of trametinib, sotorasib, encorafenib, dabrafenib and vemurafenib on ERK1/2 activation in all the cell lines tested (i.e., Fig. 4A-B, compare lanes #4 and #6). The addition of anti-EGF VacAbs reversed the deleterious effect of hEGF and, as a result, the combination of the antibodies with the inhibitors effectively suppressed the activation of pERK1/2 in KRAS, NRAS and BRAF-mut cells (i.e., Fig. 4A-B, compare lanes #6 and #7). The anti-EGFR monoclonal antibodies cetuximab and panitumumab were found to exert similar effects when combined with BRAFi and sotorasib, respectively (Fig. 4B-C, Supplementary Fig. 17B). The results obtained in the case of inhibitors of the Akt pathway were less conclusive (Supplementary Fig. 17C-D).

**Anti-EGF VacAbs delayed the appearance of resistant colonies to inhibitors targeting the MAPK/ERK and PI3K/Akt pathways**

As previously mentioned, activation of the EGFR pathway is associated with acquired resistance to a wide variety of small molecule

inhibitors of signal transduction proteins [22–27]. In consequence, we investigated the effects of hEGF and anti-EGF VacAbs on the emergence of resistant colonies to drugs targeting the MAPK/ERK and PI3K/Akt pathways. To this end, low confluence cell cultures growing in 96-well plates were treated with the corresponding inhibitor and/or anti-EGF VacAbs, wells were inspected three times per week and those reaching 50 % confluence were scored as positive.

First, we observed that hEGF at 0.1 to 10 ng/mL significantly accelerated the appearance of colonies resistant to encorafenib in the BRAF-mut HT29 cells (Supplementary Fig. 18A). Conversely, we found that the addition of anti-EGF VacAbs to the culture medium significantly delayed the *in vitro* emergence of resistance to trametinib in DLD1 and LS174T, encorafenib in HT29, vemurafenib in WM115, and capivasertib and copanlisib in NCI-H508 cells (Fig. 5); while relatively minor, no-significant effects were observed in other cases (Supplementary Fig. 18B). We also performed head-to-head comparisons of anti-EGF VacAbs with anti-EGFR monoclonal antibodies in this setting. We found that panitumumab and anti-EGFR VacAbs induced a modest, non-significant delay in the emergence of resistance to sotorasib in NCI-H23 (Supplementary Fig. 18C). In contrast, significant effects were observed in the case of HT29 cells and encorafenib, where anti-EGF VacAbs were found to be more potent than cetuximab in preventing the emergence of resistance in presence of hEGF. Resistant colonies appeared in >50 % of wells after 20–25 days of treatment with encorafenib single agent, 30–40 days in presence of cetuximab and >60 days if anti-EGF VacAbs were added to the medium (Fig. 5C).

**Colonies resistant to encorafenib or the combinations with cetuximab and anti-EGF VacAbs showed different phospho-protein and gene expression patterns**

After the emergence of resistant clones to encorafenib (ER), encorafenib combined with cetuximab (ECR) and encorafenib with anti-EGF VacAbs (EAR) (Fig. 5C), we isolated ten HT29-derived colonies per treatment, as described in methods. To gain insight into possible mechanisms of resistance, the isolated colonies were characterized at the DNA, RNA, and protein levels. NGS using a panel targeting mutations and copy number variations in 30 genes frequently altered in lung cancer including EGFR, KRAS, NRAS, PIK3CA or MET (Supplementary Table 5) did not detect any differences between the genotype of the parental HT29 cells and any of the resistant colonies. In Western blot experiments, five colonies resistant to encorafenib single agent showed concomitantly increased levels of pEGFR, pERK and pPRAS40 in presence of the drug, while low levels of the three phosphoproteins were found in four colonies. In contrast, high pPRAS40 with no changes in pEGFR and pERK was apparent in six colonies resistant to the combination of encorafenib plus cetuximab or anti-EGF VacAbs. Three additional colonies showed pEGFR exclusively increased for the cetuximab combined treatment vs. none for anti-EGF VacAbs, while five colonies resistant to anti-EGF VacAbs presented concomitant high levels of pErk and pPRAS40, compared to one for cetuximab (Fig. 6A-B, Supplementary Fig. 19, Supplementary Table 6).

Finally, RNA expression analysis of the resistant colonies was performed using an nCounter panel targeting 770 cancer-related genes. Frequent upregulation of the MAPK, Akt and Wnt pathways and downregulation of cell cycle genes was observed in all treatments. In contrast, upregulation of the JAK-STAT or downregulation of the Notch pathways were only apparent in colonies resistant to the combination of encorafenib with anti-EGF VacAbs, while the TGF-beta pathway only appeared upregulated in colonies resistant to encorafenib plus cetuximab and transcriptional deregulation was detected exclusively in clones resistant to encorafenib single agent (Fig. 6C-D, Supplementary Tables 7–9).

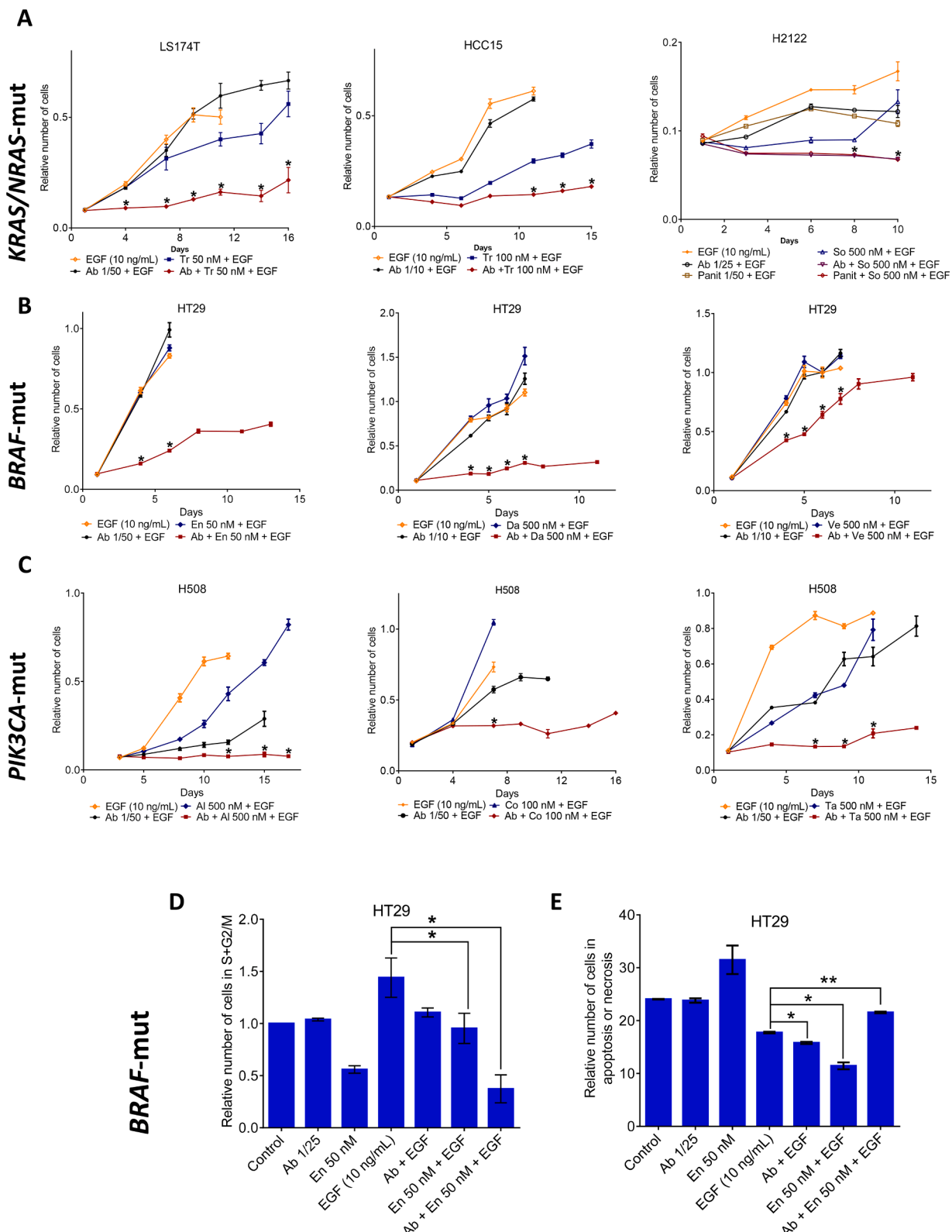


**Fig. 3.** Effects of anti-EGF VacAbs combined with inhibitors targeting the MAPK/ERK and PI3K/Akt pathways in mutant cell lines. (A-C) Growth curves at 16 days of KRAS/NRAS-mut, BRAF-mut and PIK3CA-mut cells treated with (A) MEK/G12Cis and combinations, (B) BRAFis and combinations, (C) PI3K/Aktis and combinations. (D) Percentage of HT29 cells in S + G2/M phase by flow cytometry after treatment with encorafenib, anti-EGF VacAbs and combinations. (E) Percentage of cell death in HT29 cells by annexin V analysis. Medium was RPMI+0.5 % HS in all cases. Inhibitors, hEGF and antibodies were added at the final concentrations and dilution factors indicated. \*,  $P < 0.05$  compared to hEGF treated cells (Student's t-test). Data were pooled from at least three different experiments and presented as mean  $\pm$  SEM. Ab, anti-EGF VacAbs; Al, alpelisib; Co, copanlisib; Da, dabrafenib; En, encorafenib; So, sotorasib; Ta, taselisib; Tr, trametinib; Ve, vemurafenib.

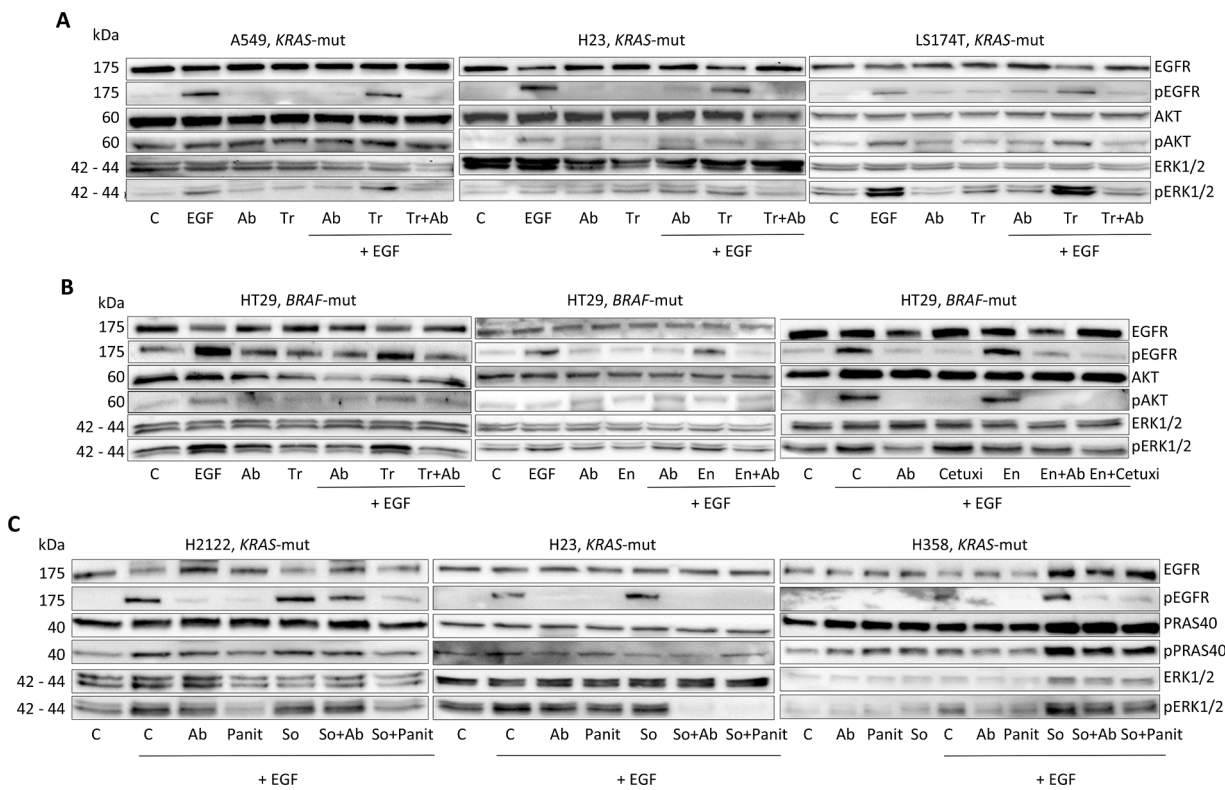


**Fig. 4.** Western blot analysis of anti-EGF VacAbs, cetuximab and panitumumab combined with inhibitors targeting the MAPK/ERK and PI3K/Akt pathways in KRAS and BRAF-mut cell lines. (A) Trametinib (1 nM) in KRAS-mut cells, (B) trametinib (10 nM) and encorafenib (50 nM) in BRAF-mut cells, (C) sotorasib (50 nM) in KRAS-mut cells. Medium was RPMI+0.5 % HS and incubation time 2 h, anti-EGF VacAbs and control antibodies were added at 1/25 dilution factor. Phospho-residues detected by Western blotting were Tyr1068 of EGFR, Ser473 of AKT, Thr202/Tyr204 of pERK1/2 and Thr246 of pPRAS40. Ab, anti-EGF VacAbs; C, control cells with no treatment; Cetuxi, cetuximab; En, encorafenib; Panit, panitumumab; So, sotorasib; Tr, trametinib. Results shown are a representative of three different experiments.

*Sera of KRAS-mut patients immunized with the anti-EGF vaccine showed lower levels of EGF and suppressed the activation in vitro of EGFR and ERK1/2*

The in vitro studies presented so far had been performed using anti-EGF VacAbs generated in rabbits, as explained in Methods. Next, we investigated sera from cancer patients who had received an anti-EGF vaccine in combination with chemotherapy in a Phase III clinical trial [30,31]. ELISA testing revealed that the levels of hEGF in the sera of KRAS-mut patients ( $n = 6$ ) dropped significantly three months after immunization with an anti-EGF vaccine, from 378.5 to 101.1 ng/mL. The same effect was observed in sera from KRAS, BRAF and PIK3CA pan-wild-type (pan-wt) individuals, decreasing from 599.6 to 159.6 ng/mL. No significant differences were observed between the two groups of patients, both of which showed high inter-individual variability (Fig. 7).

Finally, we performed experiments where A549 cultures were incubated with sera from KRAS-mut and pan-wt patients, cells collected, and pathway activation analyzed by Western blotting. We found that pre-immunization sera were unable to block hEGF-induced phosphorylation of EGFR or ERK1/2 but strongly induced Akt activation, being more potent than hEGF itself. In contrast, sera collected after three months from patients immunized with the anti-EGF vaccine reversed ERK1/2 activation while triggering Akt phosphorylation to a lesser extent than pre-immunization sera. Again, high inter-individual variation was observed (Fig. 7A, Supplementary Fig. 20).

## Discussion

The MAPK/ERK and PI3K/Akt signal transduction pathways play a

key role in human cancer and many small molecule inhibitors targeting the corresponding proteins have been developed. Some of these inhibitors have received approval for the treatment of tumors carrying mutations in specific genes involved in the two pathways (Supplementary Table 1). However, compared to other targeted therapies such as EGFR or ALK tyrosine kinase inhibitors; drugs against MAPK/ERK and PI3K/Akt pathways show higher toxicity, lower response rates and earlier emergence of resistance that reduce their clinical efficacy [6, 37–39]. To overcome these limitations, combination therapies have been tested and some of them have been FDA and EMA-approved, such as BRAFi with MEKi for BRAF-mut metastatic melanoma [19] or alpelisib with fulvestrant for PIK3CA-mut, advanced breast cancer. The EGFR and their ligands represent an attractive candidate for this type of combinatorial strategies since they are related to both intrinsic and acquired resistance to inhibitors targeting MAPK/ERK and PI3K/Akt proteins. Consequently, simultaneous blockade of EGFR signaling can improve initial response and time to relapse, as demonstrated by the trials that led to the approval of encorafenib combined with cetuximab in pretreated BRAF-mut CRC [28,29]. However, although the doublet represents an improvement over standard chemotherapy, OS is limited to 9 months and grade  $\geq 3$  adverse events appear in 57 % of patients.

Anti-EGF vaccination is an alternative to the administration of cetuximab or other anti-EGFR monoclonal antibodies (mAbs), which effectively suppresses EGFR activation and has several clinical advantages. First, it lacks toxic side-effects, as demonstrated in EPICAL trial of afatinib in combination with anti-EGF vaccination for the treatment of EGFR-mut NSCLC. No serious adverse events (SAEs) related to the vaccine were observed during the 38 months of duration of the EPICAL trial, grade  $\geq 3$  adverse events were restricted to 30 % of patients and treatment was suspended due to afatinib toxicity only in 4 % [33]. In

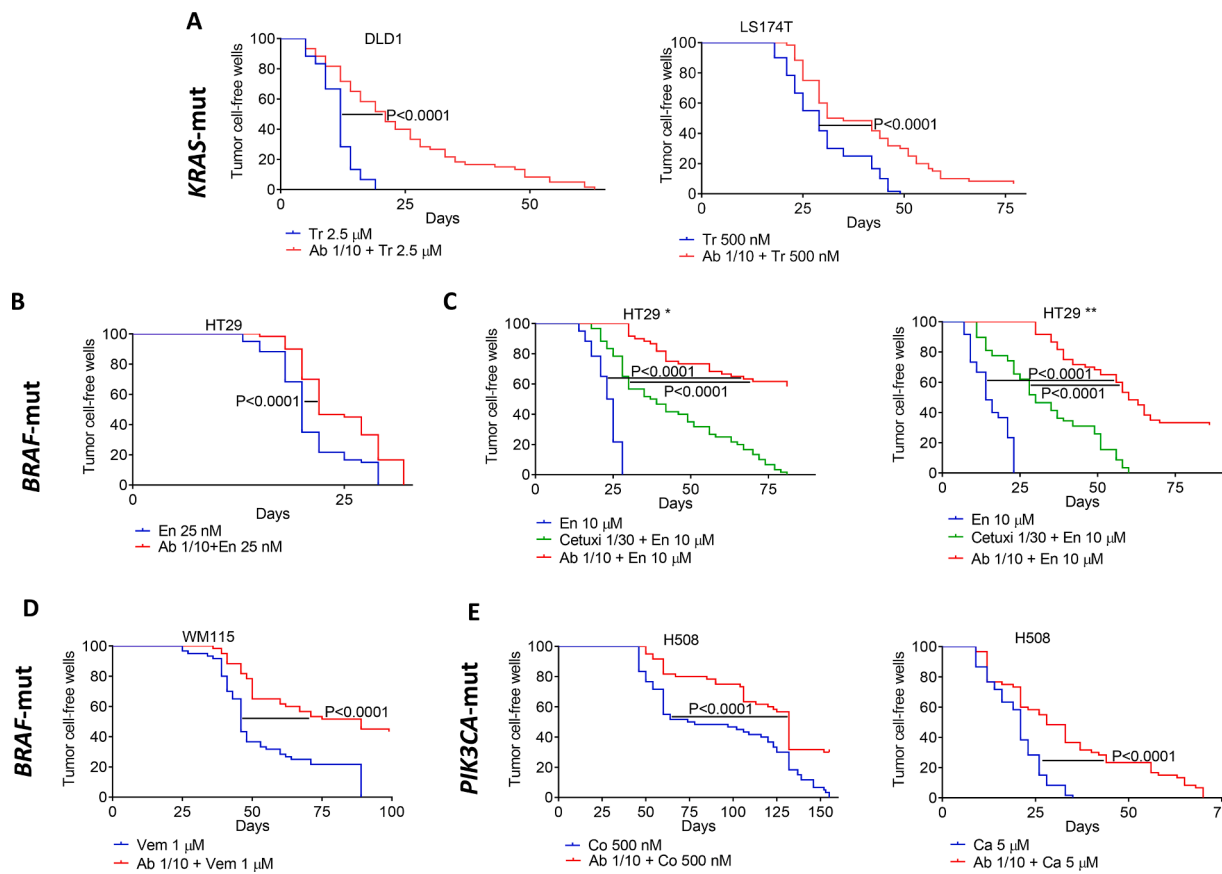


**Fig. 5.** Effects of antibodies on the emergence of colonies resistant to (A) trametinib in *KRAS*-mut cells, (B) encorafenib in *BRAF*-mut cells, (C) encorafenib with cetuximab or anti-EGF VacAbs at different hEGF concentrations, (D) vemurafenib in *BRAF*-mut cells and (E) copanlisib and capivasertib in *PIK3CA*-mut cells. Statistical significance in a Mantel-Cox test is indicated. Medium was RPMI+10 % FBS in presence of hEGF at 0.1 ng/mL (\*), 1 ng/mL (\*\*) and 10 ng/mL (no asterisks). Ab, anti-EGF VacAbs; Ca, capivasertib; Cetuxi, cetuximab; Co, copanlisib; En, encorafenib; Tr, trametinib; Vem, vemurafenib.

contrast, the phase II SWOG S1403 trial, which tested cetuximab in combination with afatinib in 174 *EGFR*-mut patients, reported 72 % of grade  $\geq 3$  adverse events, frequent dose reductions and 30 % of cetuximab discontinuation due to toxicity issues [40]. Second, anti-EGF polyclonal antibodies generated by vaccination have a significantly longer half-life compared to anti-EGFR mAbs, as demonstrated also in the EPICAL trial, >30 months compared to 4–7 days for cetuximab and panitumumab [41]. Consequently, mAbs need to be instilled intravenously to the patient weekly or biweekly for 2 h or longer periods in the day hospital; while vaccination is administered every two or three months during the maintenance period, takes less than 5 min and does not require specialized facilities or staff [33]. Third, anti-EGF vaccination induces a potent immunogenic response with high anti-EGF titers in patient's sera after three months, as demonstrated in the EPICAL trial, which persists for 30 months and can be easily monitored by a simple ELISA testing, together with the concomitant disappearance of EGF and TGF $\alpha$  in patient's serum. Of note, patients receiving corticosteroids and other immunomodulators were excluded from the EPICAL trial, since these agents can potentially interfere with immune responses. Finally, anti-EGF vaccination has the potential to equal or even outperform anti-EGFR mAbs in the clinical setting. At this respect, in the SWOG S1403 trial mentioned above, cetuximab failed to improve clinical response to afatinib (HR = 1.01; 95 % CI = 0.72 to 1.43) and the PFS for the combination was restricted to 11.9 months while, in the EPICAL trial, a PFS of 17.5 months for the combined treatment of afatinib and anti-EGF vaccination was obtained; although this result has to be considered with caution due to the small size of the trial ( $n = 23$ ).

In the first experiments of our *in vitro* study, we found a widespread reduction in the antiproliferative effects of inhibitors against MAPK/

ERK and PI3K/Akt proteins when hEGF was present in the culture medium. This observation provided us with a rationale to test the effects of anti-EGF antibodies generated by vaccination. Proliferation assays, cell cycle experiments and Western blotting results showed that, in most of the cell lines tested, anti-EGF VacAbs reversed the deleterious action of hEGF and consequently increased the antitumor activity *in vitro* of drugs targeting the MAPK/ERK and PI3K/Akt pathways. The effects of the addition of anti-EGF VacAbs were particularly intense in the case of the BRAFi, with the IC<sub>50</sub>s for encorafenib, dabrafenib and vemurafenib in presence of hEGF dropping from >2.5  $\mu$ M to 5–150 nM in the *BRAF*-mut, CRC cancer cell line HT29. Flow cytometry experiments also revealed a significant increase in G2/M arrest and cell death in HT29 cells receiving the doublet. These findings support the clinical exploration of the BRAFi combined with anti-EGF vaccination in *BRAF*-mut CRC, which should ideally be followed by a head-to-head comparison trial with cetuximab plus BRAFi, the approved treatment.

Our *in vitro* results comparing anti-EGF VacAbs vs. cetuximab also suggest that targeting EGFR activation by anti-EGF vaccination could not only equal, but even outperform, treatment with monoclonal antibodies. Thus, anti-EGF VacAbs showed a strongest beneficial effect than cetuximab on the IC<sub>50</sub>s for BRAFi (Table 1) and were significantly more potent in delaying the emergence of resistance to encorafenib treatment in CRC cells. Characterization of thirty resistant colonies also suggested some differences in the mechanisms of resistance which might explain the different activity of both antibodies. The mechanisms of resistance to cetuximab have been found to biochemically converge into MEK-ERK and AKT pathways [42], and phosphoproteomics analysis has confirmed that resistance to cetuximab in CRC is associated with increased activity of the EGFR receptor, together with the MAPK and the

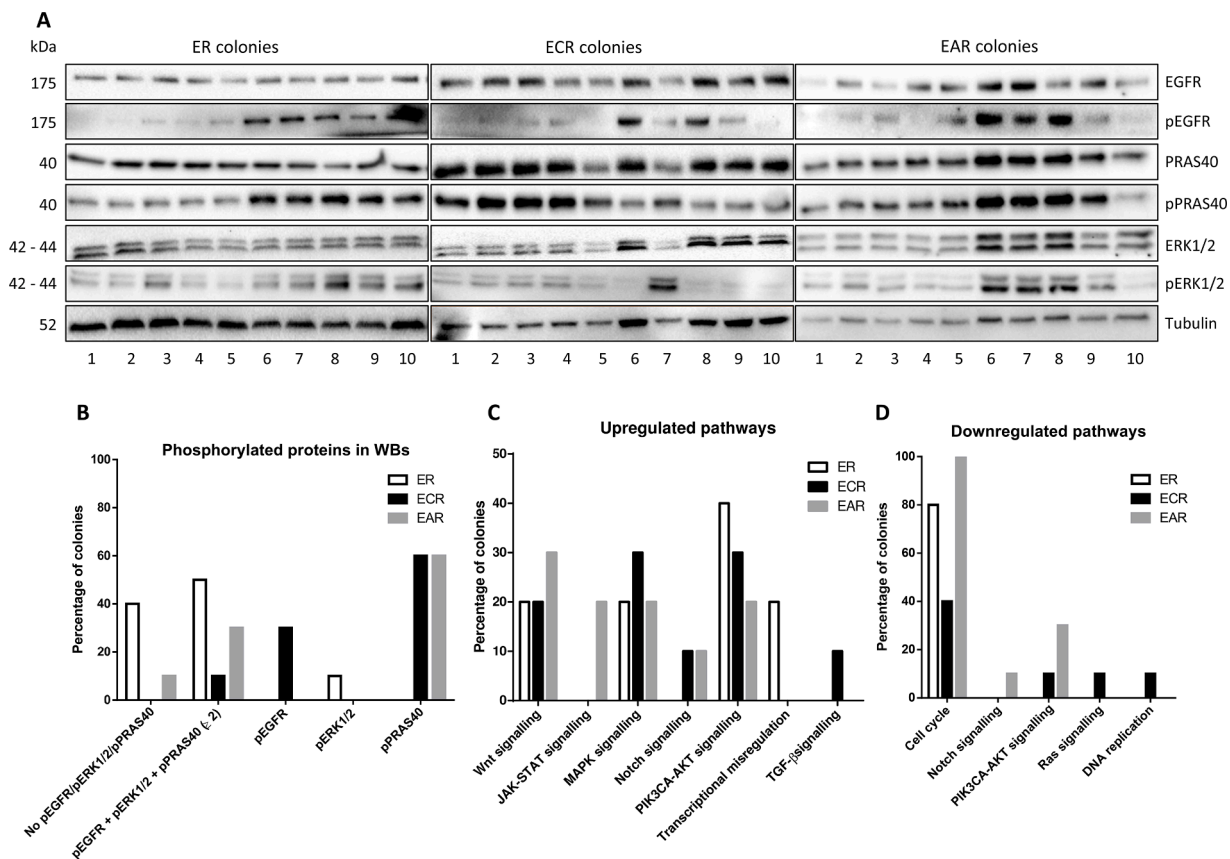


**Fig. 6.** Characterization of resistant colonies to encorafenib (ER), encorafenib combined with cetuximab (ECR) and encorafenib combined with anti-EGF VacAbs (EAR). (A) Western blot analysis of pEGFR, pERK1/2 and pPRAS40. Phospho-residues detected were Tyr1068 of EGFR, Thr202/Tyr204 of pERK1/2 and Thr246 of pPRAS40. Results shown are a representative of three different experiments. Phospho-residues detected by Western blotting were Tyr1068 of EGFR, Thr202/Tyr204 of pERK1/2 and Thr246 of pPRAS40. (B) Classification of the resistant colonies, based on the quantification from the Western blotting images presented in (A). The intensity of the bands was normalized using  $\beta$ -tubulin and compared to parental HT29 cells. (C, D) Percentage of colonies with up- and downregulated pathways, according to nCounter analysis. WB, Western blotting.

Akt pathways [43]. In our study, Western blotting for phosphoproteins revealed frequent activation of the Akt pathway in colonies resistant to combined treatment of encorafenib with both antibodies but not in those emerging after encorafenib single agent. However, activation of EGFR signaling was frequent in colonies resistant to encorafenib plus cetuximab but did not appear with the combination of encorafenib and anti-EGF VacAbs. In contrast, five colonies resistant to anti-EGF VacAbs combined with encorafenib presented concomitant high levels of pErk and pPRAS40, compared to none for cetuximab. Interestingly, nCounter results demonstrated activation of the TGF- $\beta$  pathway in colonies resistant to encorafenib plus cetuximab but not in those emerging to encorafenib and anti-EGF VacAbs treatment. Finally, nCounter also showed downregulation of the Notch and upregulation of the JAK-STAT pathways exclusively in colonies resistant to encorafenib with anti-EGF VacAbs, two mechanisms that have never been associated with resistance to cetuximab [42,43] (Fig 6C, Supplementary Table 9). Both TGF- $\beta$  and Notch pathways are strong inducers of EMT suggesting that, in contrast to cetuximab, resistance to encorafenib plus anti-EGF VacAbs could be EMT-independent [44,45].

The results obtained during our study were also remarkable in the case of sotorasib, a G12C inhibitor. Three cell lines carrying the KRAS G12C mutation were tested; NCI-H358, NCI-H2122 and NCI-H23 which showed an epithelial, mixed, and mesenchymal phenotype (Supplementary Fig. 1). Epithelial to mesenchymal transition (EMT) has been associated with intrinsic and acquired resistance to G12Ci [46] and we found that sotorasib showed a strong antiproliferative activity in NCI-H358 cells, with an IC<sub>50</sub> in the nM range; while NCI-H2122 and NCI-H23 were completely resistant to the drug (IC<sub>50</sub> > 50  $\mu$ M). The

addition of anti-EGF VacAbs strongly improved the effects of the G12Ci in mesenchymal and mixed cells, leading to an IC<sub>50</sub> of 1 nM in NCI-H2122 and 0.7  $\mu$ M in NCI-H23, while the decrease in IC<sub>50</sub> for the epithelial NCI-H358 cells was only 10-fold. Although superior to chemotherapy, sotorasib shows modest clinical activity in G12C and combination trials with other agents, including panitumumab [47], are under way. Our results suggest that the addition of anti-EGF vaccination with IN01 to G12Ci could be particularly effective in KRAS G12C-mut tumors with mesenchymal or mixed phenotype. Noteworthy, our results show that the anti-EGF VacAbs were more potent than panitumumab in head-to-head experiments in this setting (Fig. 2B, Table 1).

In summary, we have demonstrated that anti-EGF VacAbs suppress the deleterious effects of hEGF and significantly enhance the in vitro antitumor activity of targeted inhibitors in NSCLC, CRC and melanoma cell lines harboring KRAS, NRAS, BRAF and PIK3CA mutations. In combination treatment, the antibodies also delay the emergence of resistant clones and effectively block hEGF-induced activation of EGFR downstream pathways. Based on these findings; phase I trials of anti-EGF vaccination with IN01 in combination with inhibitors targeting the MAPK/ERK and PI3K/Akt pathways are warranted. One of such trials (vaccination plus encorafenib in BRAF-mut CRC patients) has already been approved by the regulatory agencies of two European countries.

#### CRediT authorship contribution statement

**Silvia García-Roman:** Investigation, Methodology, Data curation, Formal analysis, Writing – original draft, Writing – review & editing.

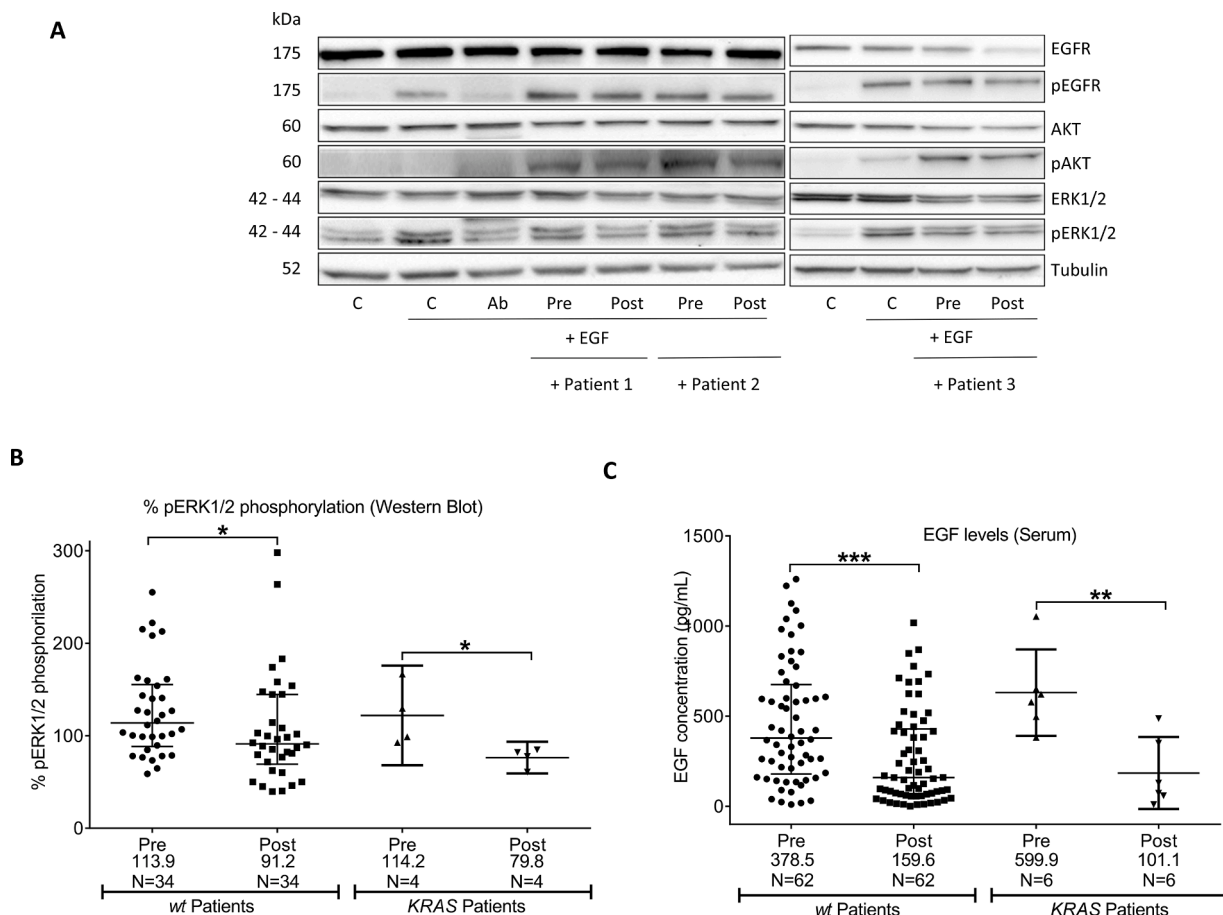


**Fig. 7.** Analysis of sera collected after three months from KRAS-mut and wild-type (wt) patients receiving an anti-EGF vaccine. (A) Western blot analysis of selected markers in KRAS-mut A549 cells treated with KRAS-mut patient's sera, collected preimmunization (Pre) and postimmunization (Post), three months after first injection. Medium was RPMI+0.5 % HS and incubation time 2 h. Phospho-residues detected by Western blotting were Tyr1068 of EGFR, Ser473 of AKT and Thr202/Tyr204 of pERK1/2. (B) Levels of pERK1/2 in A549 cells treated with sera from wt or KRAS-mut patients, as estimated by Western blotting analysis. The intensity of the bands was normalized using total ERK1/2. Horizontal bars represent medians and error bars interquartile range. \* $p < 0.05$  in a Mann-Whitney U test. (C) Levels of EGF in the sera of wt vs. KRAS-mut immunized patients. Horizontal bars represent medians and error bars interquartile range. \*\* $p < 0.01$  and \*\*\* $p < 0.001$  in a Mann-Whitney U test is indicated.

**Mónica Garzón-Ibáñez:** Investigation, Methodology, Data curation, Writing – review & editing. **Jordi Bertrán-Alamillo:** Investigation, Methodology, Data curation, Writing – review & editing. **Núria Jordana-Ariza:** Investigation, Methodology, Data curation, Writing – review & editing. **Ana Giménez-Capitán:** Investigation, Methodology, Data curation, Writing – review & editing. **Beatriz García-Peláez:** Investigation, Methodology, Data curation, Writing – review & editing. **Marta Vives-Usano:** Investigation, Methodology, Data curation, Writing – review & editing. **Jordi Codony-Servat:** Investigation, Methodology, Data curation, Writing – review & editing. **Erik d'Hondt:** Supervision, Project administration, Funding acquisition, Writing – review & editing. **Rafael Rosell:** Supervision, Project administration, Writing – review & editing. **Miguel Ángel Molina-Vila:** Investigation, Methodology, Data curation, Formal analysis, Supervision, Writing – original draft, Writing – review & editing.

#### Declaration of competing interest

Dr. d'Hondt is a full-time employee of IN3BIO. Dr d'Hondt has a patent Methods and compositions for inhibition of EGF/EGFR pathway in combination with tyrosine kinase inhibitors pending to IN3BIO. All remaining authors have declared no conflicts of interest.

#### Acknowledgments

We thank Isabel Crespo and Sara Ozcoz from the Cytomics Core Facility of the Institut d'Investigacions Biomèdiques August Pi i Sunyer (IDIBAPS) for technical assistance. The study was funded by grants from IN3BIO.

#### Supplementary materials

Supplementary material associated with this article can be found, in the online version, at [doi:10.1016/j.tranon.2024.101878](https://doi.org/10.1016/j.tranon.2024.101878).

#### References

- [1] M. Aldea, L. Friboulet, S. Apcher, F. Jaulin, F. Mosele, T. Sourisseau, et al., Precision medicine in the era of multi-omics: can the data tsunami guide rational treatment decision? *ESMO Open* 8 (2023) 101642.
- [2] J.G. Tate, S. Bamford, H.C. Jubb, Z. Sondka, D.M. Beare, N. Bindal, et al., COSMIC: the catalogue of somatic mutations in cancer, *Nucl. Acids. Res.* 47 (2019) D941–D97.
- [3] M. Zhang, H. Jang, R. Nussinov, PI3K driver mutations: a biophysical membrane-centric perspective, *Cancer Res.* 81 (2021) 237–247.
- [4] G. Kim, A.E. McKee, Y.M. Ning, M. Hazarika, M. Theoret, J.R. Johnson, et al., FDA approval summary: vemurafenib for treatment of unresectable or metastatic melanoma with the BRAFV600E mutation, *Clin. Cancer Res.* 20 (2014) 4994–5000.
- [5] A.D. Ballantyne, K.P. Garnock-Jones, Dabrafenib: first global approval, *Drugs* 73 (2013) 1367–1376.

[6] A. Hauschild, J.J. Grob, L.V. Demidov, T. Jouary, R. Gutzmer, M. Millward, et al., Dabrafenib in BRAF-mutated metastatic melanoma: a multicentre, open-label, phase 3 randomised controlled trial, *Lancet* 380 (2012) 358–365.

[7] G.R. Blumenschein Jr, E.F. Smit, D. Planchard, D.W. Kim, J. Cadranel, T. De Pas, et al., A randomized phase II study of the MEK1/MEK2 inhibitor trametinib (GSK1120212) compared with docetaxel in KRAS-mutant advanced non-small-cell lung cancer (NSCLC) [dagger], *Ann. Oncol.* 26 (2015) 894–901.

[8] J.R. Infante, B.G. Somer, J.O. Park, C.P. Li, M.E. Scheulen, S.M. Kasabhai, et al., A randomised, double-blind, placebo-controlled trial of trametinib, an oral MEK inhibitor, in combination with gemcitabine for patients with untreated metastatic adenocarcinoma of the pancreas, *Eur. J. Cancer* 50 (2014) 2072–2081.

[9] L.S. Rosen, P. LoRusso, W.W. Ma, J.W. Goldman, A. Weise, A.D. Colevas, et al., A first-in-human phase I study to evaluate the MEK1/2 inhibitor, cobimetinib, administered daily in patients with advanced solid tumors, *Invest. New Drugs* 34 (2016) 604–613.

[10] E.C. Nakajima, N. Drezner, X. Li, P.S. Mishra-Kalyani, Y. Liu, H. Zhao, et al., FDA approval summary: sotorasib for KRAS G12C-mutated metastatic NSCLC, *Clin. Cancer Res.* 28 (2022) 1482–1486.

[11] S. Dhillon, Adagrasib: first approval, *Drugs* 83 (2023) 275–285.

[12] F. Skoulidis, B.T. Li, G.K. Dy, T.J. Price, G.S. Falchook, J. Wolf, et al., Sotorasib for lung cancers with KRAS p.G12C mutation, *N. Engl. J. Med.* 384 (2021) 2371–2381.

[13] P.A. Janne, G.J. Riely, S.M. Gadgeel, R.S. Heist, S.I. Ou, J.M. Pacheco, et al., Adagrasib in non-small-cell lung cancer harboring a KRAS(G12C) mutation, *N. Engl. J. Med.* 387 (2022) 120–131.

[14] V.E. Kwirkowski, T.M. Prowell, A. Ibrahim, A.T. Farrell, R. Justice, S.S. Mitchell, et al., FDA approval summary: temsirolimus as treatment for advanced renal cell carcinoma, *Oncologist* 15 (2010) 428–435.

[15] P.J. Houghton, Everolimus, *Clin. Cancer Res.* 16 (2010) 1368–1372.

[16] A. Markham, Copanlisib: first global approval, *Drugs* 77 (2017) 2057–2062.

[17] B.W. Miller, D. Przepiorka, R.A. de Claro, K. Lee, L. Nie, N. Simpson, et al., FDA approval: idelalisib monotherapy for the treatment of patients with follicular lymphoma and small lymphocytic lymphoma, *Clin. Cancer Res.* 21 (2015) 1525–1529.

[18] A. Andrikopoulou, S. Chatzinikolaou, E. Panourgias, M. Kaparelou, M. Lontos, M. A. Dimopoulos, et al., The emerging role of capivasertib in breast cancer, *Breast* 63 (2022) 157–167.

[19] Combination therapy approved for melanoma, *Cancer Discov.* 4 (2014) 262.

[20] L. Odogwu, L. Mathieu, G. Blumenthal, E. Larkins, K.B. Goldberg, N. Griffin, et al., FDA approval summary: dabrafenib and trametinib for the treatment of metastatic non-small cell lung cancers harboring BRAF V600E mutations, *Oncologist* 23 (2018) 740–745.

[21] P. Narayan, T.M. Prowell, J.J. Gao, L.L. Fernandes, E. Li, X. Jiang, et al., FDA approval summary: alpelisib plus fulvestrant for patients with HR-positive, HER2-negative, PIK3CA-mutated, advanced or metastatic breast cancer, *Clin. Cancer Res.* 27 (2021) 1842–1849.

[22] A.J. Cooper, L.V. Sequist, J.J. Lin, Third-generation EGFR and ALK inhibitors: mechanisms of resistance and management, *Nat. Rev. Clin. Oncol.* 19 (2022) 499–514.

[23] G. Recondo, M. Bahcall, L.F. Spurr, J. Che, B. Ricciuti, G.C. Leonardi, et al., Molecular mechanisms of acquired resistance to MET tyrosine kinase inhibitors in patients with MET exon 14-mutant NSCLC, *Clin. Cancer Res.* 26 (2020) 2615–2625.

[24] J.F. Gainor, L. Dardaei, S. Yoda, L. Friboulet, I. Leshchiner, R. Katayama, et al., Molecular mechanisms of resistance to first- and second-generation ALK inhibitors in ALK-rearranged lung cancer, *Cancer Discov.* 6 (2016) 1118–1133.

[25] A. Passaro, P.A. Janne, T. Mok, S. Peters, Overcoming therapy resistance in EGFR-mutant lung cancer, *Nat. Cancer* 2 (2021) 377–391.

[26] J. Zhou, Q. Ji, Q. Li, Resistance to anti-EGFR therapies in metastatic colorectal cancer: underlying mechanisms and reversal strategies, *J. Exp. Clin. Cancer Res.* 40 (2021) 328.

[27] J. Pastwinska, K. Karas, I. Karwaciak, M. Ratajewski, Targeting EGFR in melanoma - the sea of possibilities to overcome drug resistance, *Biochim. Biophys. Acta Rev. Cancer* 1877 (2022) 188754.

[28] S. Kopetz, A. Grothey, R. Yaeger, E. Van Cutsem, J. Desai, T. Yoshino, et al., Encorafenib, binimetinib, and cetuximab in BRAF V600E-mutated colorectal cancer, *N. Engl. J. Med.* 381 (2019) 1632–1643.

[29] J. Tabernero, A. Grothey, E. Van Cutsem, R. Yaeger, H. Wasan, T. Yoshino, et al., Encorafenib plus cetuximab as a new standard of care for previously treated BRAF V600E-mutant metastatic colorectal cancer: updated survival results and subgroup analyses from the BEACON study, *J. Clin. Oncol.* 39 (2021) 273–284.

[30] R. Rosell, E. Neninger, M. Nicolson, R.M. Huber, S. Thongprasert, P.M. Parikh, et al., Pathway targeted immunotherapy: rationale and evidence of durable clinical responses with a novel, EGF-directed agent for advanced NSCLC, *J. Thorac. Oncol.* 11 (2016) 1954–1961.

[31] J. Codony-Servat, S. García-Roman, M.A. Molina-Vila, J. Bertran-Alamillo, A. Gimenez-Capitan, S. Viteri, et al., Anti-epidermal growth factor vaccine antibodies enhance the efficacy of tyrosine kinase inhibitors and delay the emergence of resistance in EGFR mutant lung cancer cells, *J. Thorac. Oncol.* 13 (2018) 1324–1337.

[32] J. Codony-Servat, S. García-Roman, M.A. Molina-Vila, J. Bertran-Alamillo, S. Viteri, E. d'Hondt, et al., Anti-epidermal growth factor vaccine antibodies increase the antitumor activity of kinase inhibitors in ALK and RET rearranged lung cancer cells, *Transl. Oncol.* 14 (2021) 100887.

[33] D. Rodriguez-Abreu, M. Cobo, S. García-Roman, S. Viteri-Ramirez, N. Jordana-Ariza, B. García-Pelaez, et al., The EPICAL trial, a phase Ib study combining first line afatinib with anti-EGF vaccination in EGFR-mutant metastatic NSCLC, *Lung Cancer* 164 (2022) 8–13.

[34] C. Aguado, C. Teixido, R. Roman, R. Reyes, A. Gimenez-Capitan, E. Marin, et al., Multiplex RNA-based detection of clinically relevant MET alterations in advanced non-small cell lung cancer, *Mol. Oncol.* 15 (2021) 350–363.

[35] C. Verges, A. Gimenez-Capitan, V. Ribas, J. Salgado-Borges, F. March de Ribot, C. Mayo-de-Las-Casas, et al., Gene expression signatures in conjunctival fornix aspirates of patients with dry eye disease associated with Meibomian gland dysfunction. A proof-of-concept study, *Ocul. Surf.* 30 (2023) 42–50.

[36] Y. Kuboki, R. Yaeger, M. Fakih, J.H. Strickler, T. Masuishi, E.J-H. Kim, et al., 45MO Sotorasib in combination with panitumumab in refractory KRAS G12C-mutated colorectal cancer: safety and efficacy for phase Ib full expansion cohort, *Ann. Oncol.* 33 (2022) S1445–S1446, <https://doi.org/10.1016/j.annonc.2022.10.077>.

[37] D.S. Hong, M.G. Fakih, J.H. Strickler, J. Desai, G.A. Durm, G.I. Shapiro, et al., KRAS(G12C) inhibition with sotorasib in advanced solid tumors, *N. Engl. J. Med.* 383 (2020) 1207–1217.

[38] J.H. Strickler, H. Satake, T.J. George, R. Yaeger, A. Hollebecque, I. Garrido-Laguna, et al., Sotorasib in KRAS p.G12C-mutated advanced pancreatic cancer, *N. Engl. J. Med.* 388 (2023) 33–43.

[39] P.B. Chapman, A. Hauschild, C. Robert, J.B. Haanen, P. Ascierto, J. Larkin, et al., Improved survival with vemurafenib in melanoma with BRAF V600E mutation, *N. Engl. J. Med.* 364 (2011) 2507–2516.

[40] S.B. Goldberg, M.W. Redman, R. Lilienbaum, K. Politi, T.E. Stinchcombe, L. Horn, et al., Randomized trial of afatinib plus cetuximab versus afatinib alone for first-line treatment of EGFR-mutant non-small-cell lung cancer: final results from SWOG S1403, *J. Clin. Oncol.* 38 (2020) 4076–4085.

[41] J.M. Hubbard, S.R. Alberts, Alternate dosing of cetuximab for patients with metastatic colorectal cancer, *Gastrointest. Cancer Res.* 6 (2013) 47–55.

[42] V. Sforza, E. Martinelli, F. Ciardiello, V. Gambardella, S. Napolitano, G. Martini, et al., Mechanisms of resistance to anti-epidermal growth factor receptor inhibitors in metastatic colorectal cancer, *World J. Gastroenterol.* 22 (2016) 6345–6361.

[43] R. Beekhof, A. Bertotti, F. Bottger, V. Vurchio, F. Cottino, E.R. Zanella, et al., Phosphoproteomics of patient-derived xenografts identifies targets and markers associated with sensitivity and resistance to EGFR blockade in colorectal cancer, *Sci. Transl. Med.* 15 (2023) eabm3687.

[44] L.A. Timmerman, J. Grego-Bessa, A. Raya, E. Bertran, J.M. Perez-Pomares, J. Diez, et al., Notch promotes epithelial-mesenchymal transition during cardiac development and oncogenic transformation, *Genes Dev.* 18 (2004) 99–115.

[45] J. Xu, S. Lamouille, R. Deryck, TGF-beta-induced epithelial to mesenchymal transition, *Cell Res.* 19 (2009) 156–172.

[46] Y. Adachi, K. Ito, Y. Hayashi, R. Kimura, T.Z. Tan, R. Yamaguchi, et al., Epithelial-to-mesenchymal transition is a cause of both intrinsic and acquired resistance to KRAS G12C inhibitor in KRAS G12C-mutant non-small cell lung cancer, *Clin. Cancer Res.* 26 (2020) 5962–5973.

[47] F. Bteich, M. Mohammadi, T. Li, M.A. Bhat, A. Sofianidi, N. Wei, et al., Targeting KRAS in colorectal cancer: a bench to bedside review, *Int. J. Mol. Sci.* 24 (2023) 12030.